



Swansea University
Prifysgol Abertawe



Cronfa - Swansea University Open Access Repository

This is an author produced version of a paper published in:

Polymer Composites

Cronfa URL for this paper:

<http://cronfa.swan.ac.uk/Record/cronfa36153>

Paper:

Korkees, F., Alston, S. & Arnold, C. (2017). Directional diffusion of moisture into unidirectional carbon fiber/epoxy Composites: Experiments and modeling. *Polymer Composites*

<http://dx.doi.org/10.1002/pc.24626>

This item is brought to you by Swansea University. Any person downloading material is agreeing to abide by the terms of the repository licence. Copies of full text items may be used or reproduced in any format or medium, without prior permission for personal research or study, educational or non-commercial purposes only. The copyright for any work remains with the original author unless otherwise specified. The full-text must not be sold in any format or medium without the formal permission of the copyright holder.

Permission for multiple reproductions should be obtained from the original author.

Authors are personally responsible for adhering to copyright and publisher restrictions when uploading content to the repository.

<http://www.swansea.ac.uk/library/researchsupport/ris-support/>

Article title:

Directional diffusion of moisture into unidirectional carbon fibre / epoxy composites:
experiments and modelling

Authors:

Feras Korkees¹, Sue Alston¹ and Cris Arnold¹

¹ Polymers and Composites Research Centre, Swansea University, Bay Campus, Swansea
SA1 8EN, Wales, United Kingdom

Corresponding Author:

Feras Korkees, Polymers and Composites Research Centre, Swansea University, Bay
Campus, Swansea SA1 8EN, Wales, United Kingdom

Email: f.a.korkees@swansea.ac.uk

Notation

C	Moisture Concentration
C^*	Relative moisture concentration
D	The molecular diffusion coefficient
D_r	Diffusivity of the matrix
D_x	Diffusion coefficient along the fibre
D_y	Diffusion coefficient across the fibres
D_z	Diffusion coefficient through the thickness
$D_{y,yarn}$	Diffusion coefficient across the yarns
$D_{z,yarn}$	Diffusion coefficient through the thickness of the yarns
$D_{yzI} (predicted)$	Predicted diffusivity in the y, and z-directions of a unit cell at microscale
$D_{y,composite}$	Diffusion coefficient across the composite
$D_{z,composite}$	Diffusion coefficient through the composite
h	Sample thickness
l	Sample length
M_t	Mass uptake at time t
M^*	Equilibrium mass uptake of the composite
$M^*_{,epoxy}$	Equilibrium mass uptake of the matrix
$M^*_{,fibre}$	Equilibrium mass uptake of the fibres
$M^*_{,yarn}$	Equilibrium mass uptake of the yarns
$V^f_{,fibre}$	Fibre volume fraction in the yarns
$V^f_{,yarn}$	Volume fraction of the yarns in the composite
w	Sample width

Abstract

Water diffusion into composites in different directions was examined in this study, with the aim of determining the best way of measuring diffusion coefficients and to provide values to compare with model predictions. Water absorption behaviour of unreinforced epoxy resins and carbon fibre reinforced epoxy composite materials was investigated with long-term exposure to different environmental conditions. Initial Fickian absorption was observed followed by a slower second stage that continues for at least 3.7 years. Fibre architecture was found to be an important aspect controlling absorption, where water diffusion along fibres was observed to be about three times faster than across the fibres and about seven times faster than through the thickness. A three-dimensional finite element computer model based on Fickian diffusion behaviour was developed to predict the levels of moisture absorption under hot/humid environments. A multi-scale modelling approach was used which allowed the results of simulations at the micro-structural level to be used to predict the diffusivity in different directions. The modelled diffusion coefficients showed high dependency on the detailed micro-structure. Experimental results provided a baseline for the validation of the model, and it was found that these data could be closely predicted using a reasonable micro-structure characterization.

Keywords

Carbon fibre, Directional diffusion, Moisture absorption, Multi-scale modelling.

1. Introduction

Today's ever increasing demand for lighter materials with higher strength, greater stiffness, and better reliability has led to extensive research on and development of composite materials. Structural composites are usually subjected to a range of environmental conditions through their service life leading to plasticization of the resin and reductions in some properties. In hot/wet environments, there is still uncertainty of the long term stability of composites, in which moisture can diffuse easily and rapidly into polymers in early stages followed by a slow gradual increase in the second stage until finally moisture reaches an equilibrium concentration and thus material saturates. Diffusion of moisture into thick components is normally a slow process. Even though the kinetics of moisture absorption start almost immediately on contact with the environment within the surface layers, it may take weeks to months before a considerable amount of moisture has been absorbed by the composite, and considerably longer periods (i.e. 1-2 years) before the material is saturated [1].

A Fickian diffusion process in which saturation reaches constant values has been commonly used in most methods to account for the rate of moisture absorption. On the contrary, a slow steady increase in moisture content beyond the initial Fickian period in epoxy resin based composites has been reported in several studies. Water uptake in unidirectional carbon fibre /epoxy composites was studied [2]. The results showed two-stage diffusion with the first stage following Fickian behaviour and

relaxation/deterioration dominating the second stage. Two different absorption stages were distinguished [3] when unidirectional composites were investigated under hygrothermal environments. In the first stage, Fickian behaviour was noticed at short time, where the capillary diffusion was negligible at the interface and molecular diffusion through the epoxy matrix dominated. In the second stage, water absorption followed non Fickian water uptake at longer times, especially at high temperatures. Moreover, unidirectional graphite/epoxy composites exhibited a mixture of Fickian and non-Fickian diffusion behaviour when the materials were subjected to water at various temperatures for long period of time [4].

An important aspect that can affect the diffusion mechanism is the fibre architecture. This is essential to consider where edge surfaces are exposed to moisture. It has been reported by many researchers that water access along fibres is faster than across fibres. The moisture diffusion coefficient of carbon fibre/epoxy composites taking into account the anisotropy of the material was studied [5]. It was found that moisture uptake followed Fickian behaviour and diffusion along the fibres was 2-4 times larger than diffusion in both the transverse direction and the thickness direction. The diffusion in the fibre direction was also found to be 20 times faster than that in the transverse direction, which implies water tends to penetrate along the fibre whereas carbon fibre does not absorb water [6]. This difference was explained to be due to the complicated path in the transverse direction that water molecules follow to move around the fibres [7].

Generally, there is a need to improve design capabilities for carbon / epoxy composites with long-term and transient exposure to humid environments. A better design capability will lead to safe reductions in component sizes with consequent weight reductions and environmental savings. Therefore, there is a need to accurately model the ingress of water into composites, to avoid very time-consuming component testing. Consequently, the determination of the mechanisms of water diffusion and the detailed modelling of water uptake can allow improved design. With rapidly growing computational modelling capability, the micromechanical analysis of fibre reinforced composite materials has become an important means of understanding the behaviour of these materials. For the reason, CAD software, finite element analysis and predictive modelling methods have been increasingly used to give information on the influences of the environment on polymer composite materials, and special analytical formulations have also been developed for this purpose.

Modelling of moisture absorption into polymer composites depends considerably on the diffusion laws used. The majority of the models developed over the years for describing the water diffusion mechanism in polymer composite materials are based on Fick's laws. The one-dimensional Fickian model is used frequently to model diffusion of water in a homogeneous material and where there is no chemical interaction between the absorbed water and the material [8,9].

Finite element calculations were performed to simulate moisture diffusion for 1, 2 and 4 mm thick samples. The agreement between the FEM model and the experiment was reasonably good only for short and medium periods of time. This is because the specimens with various thicknesses didn't reach equilibrium. In addition, the edge effect

was taken into account in this model because the specimen geometry governs the moisture diffusion data. It was observed that when neglecting the edge effect by testing very thin specimens, a numerical error was produced leading to a significant distortion of the actual moisture diffusion data [10]. A three-dimensional finite element model was also used to study the water diffusion behaviour of CFRP laminates [6]. The governing equation for diffusion analysis was an extension of Fick's law. Predictions showed that the diffusivity in the fibre direction is much larger than that in the transverse direction.

This work aimed to investigate the directional diffusion in unidirectional carbon fibre/epoxy composites, derive the directional diffusivity from measured data using different methods to account for edge effects, and finally model and validate diffusion through a detailed UD composite structure. The experimental curves and diffusivity ratios were compared with predictions from FE modelling at two scales based on the detailed microstructure.

2. Materials and conditioning

Composite samples comprising T800S Carbon fibres and M21 epoxy resin were manufactured into unidirectional lay-up sheets generally of 25 mm thickness (132 plies) using conventional autoclave processing. The composite panels passed ultrasonic inspection and volume fraction measurements showed them to have a V_f of 58% with a void content of less than 0.2%. In order to understand the effects of fibre orientations and arrangements on diffusion, these UD sheets were cut into samples with various thicknesses in three different orientations: along the fibres, across the layers and through

the thickness which are shown in Figure 1 as 1, 2 and 3 respectively. The specimens needed to be relatively thin so that diffusion into the specimen was mainly through the largest surfaces and to ensure that diffusion through the smaller surfaces was negligible, hence reducing the ‘edge effects’. Specimens with various thicknesses were used to examine the edge effects and thickness effects on the diffusion rate.

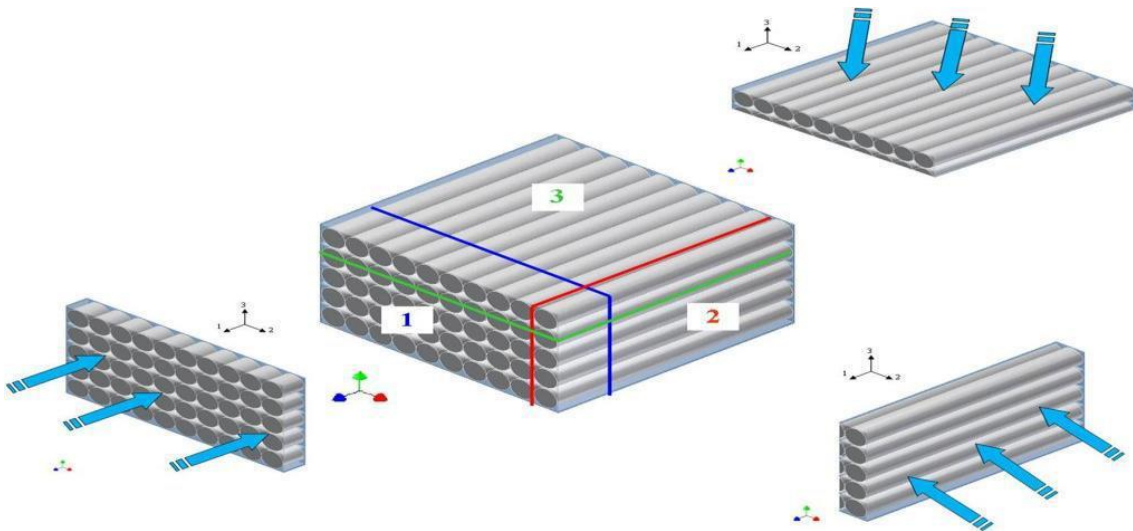


Figure 1. UD orientations.

Samples were prepared from these sheets by water-jet cutting into blocks followed by accurate sectioning with a metallographic diamond saw. Sets of samples were cut with the thin dimension in the 1, 2 and 3 directions respectively. All samples were approximately 25mm x 25mm in size with a thickness of 1, 2 or 4mm. A total of 90 separate samples were cut, where two samples of each thickness in each of the three orientations were tested in five moisture absorption conditions. Cut surfaces of samples

were investigated using optical microscopy and SEM and no observable damage such as micro-cracks were evident due to either the water-jet cutting or diamond saw sectioning (Figure 2). After the cutting procedure, samples were abraded with 1200 grit abrasive paper to remove any pronounced saw striations and smooth damaged edges. Unreinforced resin samples of the same material were supplied by the materials manufacturer with dimensions of 33mm x 19.9mm x 4mm.

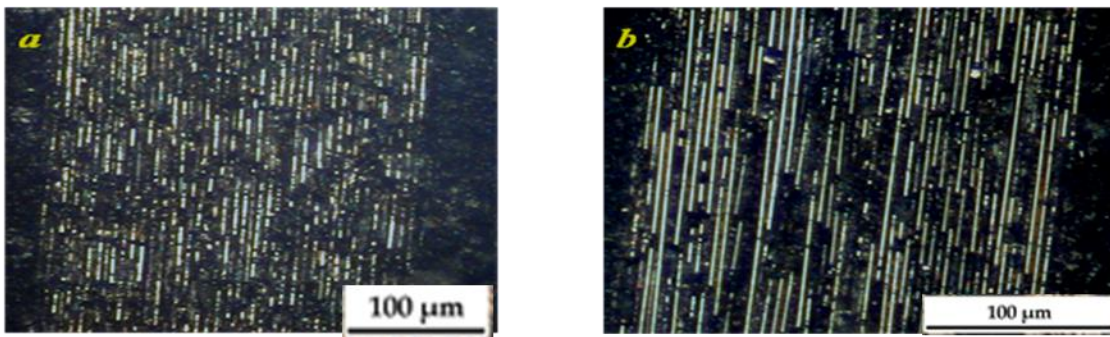


Figure 2. Optical micrographs for samples after a) water jet cutting and b) diamond saw cutting.

3. Directional diffusion of water into composites

It is well established that the rate of diffusion can be very dependent on direction in fibre-composites [5-10]. This is due to the anisotropic nature of most carbon fibre composites which leads to anisotropic water diffusion behaviour. Generally, if the thickness of the composite is large compared to the other dimensions, moisture entering through the edges has to be taken into account if the edges do not have a moisture-impermeable coating. Diffusion in general is fast along the fibre direction with slower diffusion through the thickness of the composite. This can be attributed mainly to the difference in diffusion

paths with shorter paths possible along the fibres, though there may also be effects due to the interphase or debonding along the fibres. In order to be able to model or predict behaviour accurately in service, this directionality must be taken into account [11].

Table 1 summaries some of the previous studies that have considered this effect using various materials, different fibre arrangements, and various methods to measure the directional diffusion behaviour. All methods used measure water uptake in certain directions and monitor weight changes during conditioning. These studies show that the ratio of longitudinal to transverse diffusion coefficient has been measured as anything between 2 and 24. Being able to measure the different diffusion rates is important for any modelling of water uptake, and since there will be some differences from material to material, a robust method of measuring the difference is needed.

Table 1: Directional diffusion constants of carbon fibre/epoxy resin composites from previous studies

Author(s)	Material	Direction	M^* %	D ($\times 10^{-14}$ m ² /s)
(Leung, 1979) [16]	AS/3501-5 graphite/epoxy composites	Along	-	162
		Across		68
		Through		63
(Arao,	Unidirectional	Along		154

2007) [5]	carbon fibre/epoxy composites	Across Through	1.3	68 36
(Aoki, 2008) [6]	T800H/3633 carbon fibre/epoxy laminates	Fibre direction Transverse direction	1.73- 1.74	803 32.5

Initially, in this study attempts were made to seal up the edges of composite samples, using adhesive-backed foil tape and vacuum-deposited thin layers of aluminum. In all cases, some water was found to penetrate the sealed material and so these methods could not be used reliably. Therefore, as it was believed that edge effects would be important, specimens of different thickness with directions along the fibres, across the layers or through the thickness were tested to determine the directional diffusion coefficients.

4. Conditioning and measurements

Specimens were first dried in an oven at 70 °C until the specimen weights were stabilized before conducting the absorption experiments. All unidirectional and resin specimens were conditioned in water at 23, 40 and 70 °C, and also in 45%, 60% and 85 % RH at 70 °C. The weight gain of the specimens was carefully monitored by weighing them periodically at increasing intervals using a balance with a resolution of 0.01 mg. and the percentage weight gain, $W\%$, was determined.

The weight gain of each sample was plotted against the square root of time with the expectation that the samples would show Fickian behaviour and so the first part of this graph would be linear. Figure 3 (top) shows the effect of sample thickness for the through-thickness samples for the same condition. Figure 3 (bottom) shows the effect of direction for 2mm thick samples conditioned in 70°C water. These graphs show features that are not too surprising. The thicker samples have a slower weight uptake, and the samples with the thin dimension along the fibres have a faster uptake than those cut across the fibres which is faster than those cut through the layers.

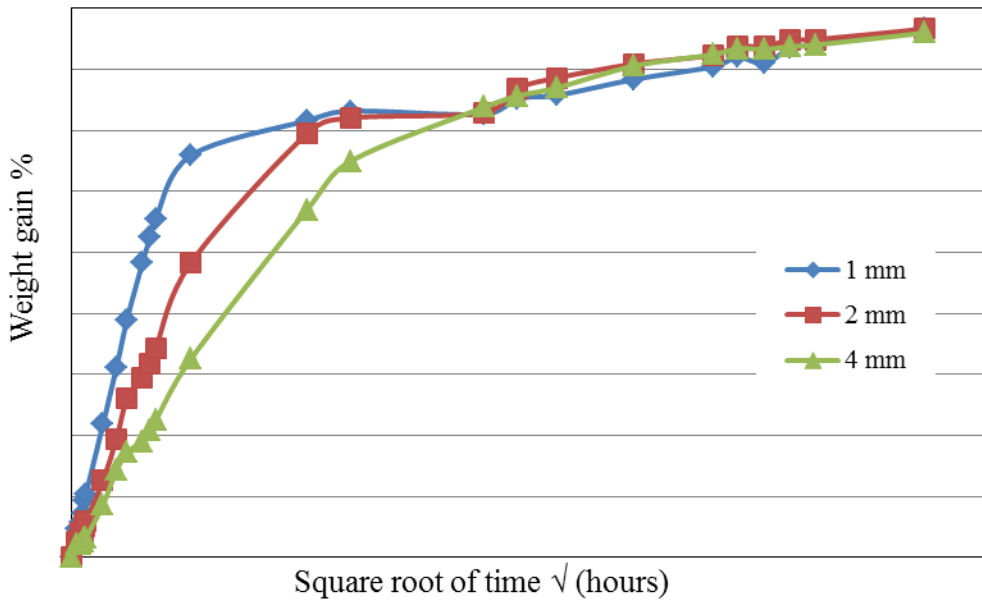
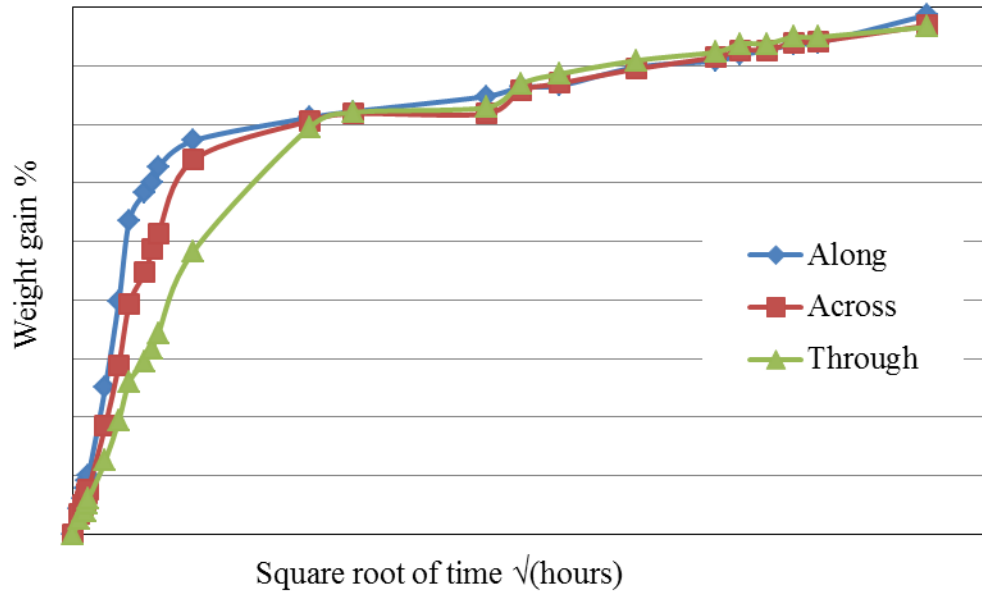


Figure 3. Water uptake curves through the thickness of carbon fibre/M-21 epoxy composite specimens in water at 70 °C (top). Water uptake curves for different orientations carbon fibre/M-21 epoxy composite specimens with 2mm thickness in water at 70 °C (bottom).

Diffusion in general is a thermo-active process and the diffusion coefficient is very sensitive to temperature of immersion. This temperature dependency can be expressed by the Arrhenius equation, where diffusion coefficients show a linear relation when plotted in terms of $\ln(D)$ versus $1/T$ as shown in Figure 4 which shows that increasing the temperature accelerates short term diffusion and increases the diffusion coefficient.

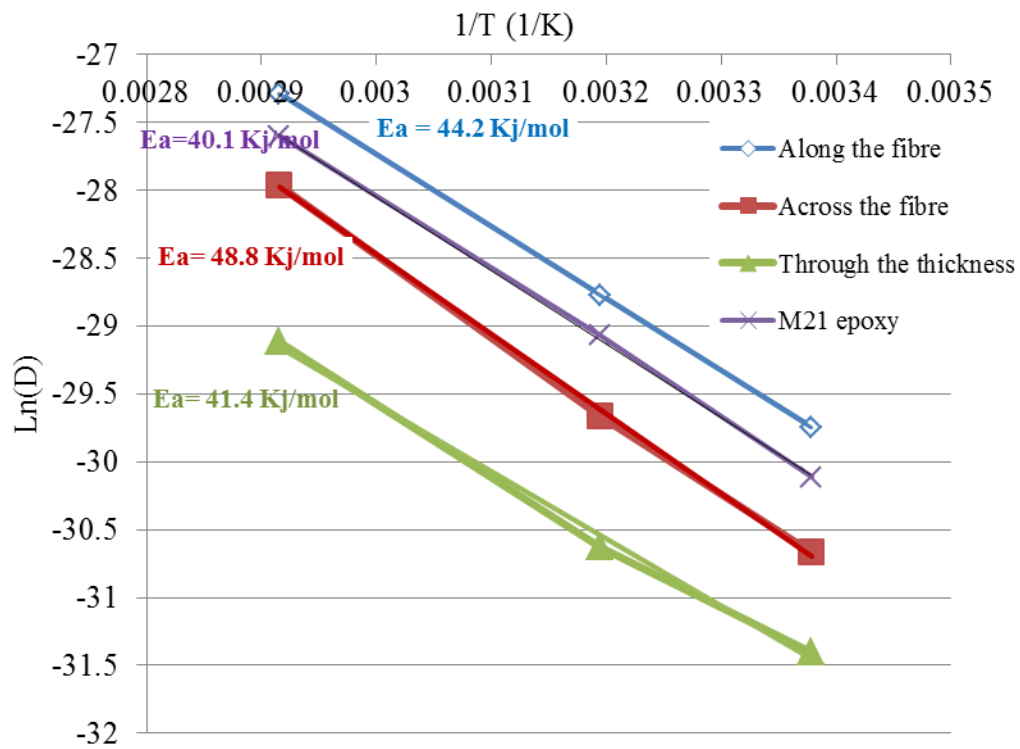


Figure 4. Arrhenius plots for the Fickian diffusion values.

According to Arrhenius equation, the diffusion coefficient is dependent on the activation energy which is expected to be the same for composites with impermeable fibres and

pure resin. Generally, the activation energies of the resin and its composites should be the same if water diffusion through the matrix was the only mechanism of water penetration [12]. The activation energy can be calculated from the slopes in Figure 4 and this shows that there are some differences in activation energy between materials. The values for the neat resin seem to be slightly lower than for the composites, suggesting that the presence of the fibres may hinder water movement through the resin, possibly by providing additional constraints to polymer chain movement. The reason for this behaviour was given by Bao (2002) [13] who concluded that the rigid carbon fibre surface may apply constraints on segmental motions of the matrix. The differences are not particularly large and may be due to experimental variations. The values of activation energy are similar to those found for secondary chain relaxation in epoxy resins of around 50 kJ/mol [14].

4.1 Parametric estimation technique for Fickian diffusion behaviour

Conventional Fickian diffusion curves generally level-off near the transition point at which the slope of the curve changes, and corresponds to constant moisture content beyond this [15]. However, for neat resin and the composites, even after more than 4 years of exposure, equilibrium had not been reached clearly. The long-term behaviour is reasonably well-established and it is thought to be primarily due to molecular relaxation. The FE model used in this study deals only with Fickian diffusion, so that it was necessary to extract the Fickian component of the measured data. To obtain this, the long term behaviour for resin and composites under all conditions was subtracted from the raw data, giving a value of the Fickian saturation for each sample, as illustrated in Figure 5.

For thicker samples in different directions, and those conditioned at lower temperature, it was not possible to get a good extrapolation of the long-term behaviour within the study duration. It can be assumed that the Fickian saturation is the same at each condition, regardless of sample thickness or orientation. However it was found that there was variation in V_f from sample to sample, due to the complex microstructure and relatively small sample size, and this would cause variations in the Fickian saturation for each sample. For samples that had not saturated, the following method was used.

In an attempt to handle any differences in fibre volume fraction between samples, the measured Fickian saturation values were used for all samples that did saturate. For samples that did not saturate, the average saturation values for that condition were used, but scaled by sample density as an approximate measure of the fibre volume fraction. The same fitting method was used for resin samples to deduce saturation at all conditions. The saturation values for resin and composite specimens are given in Table 2.

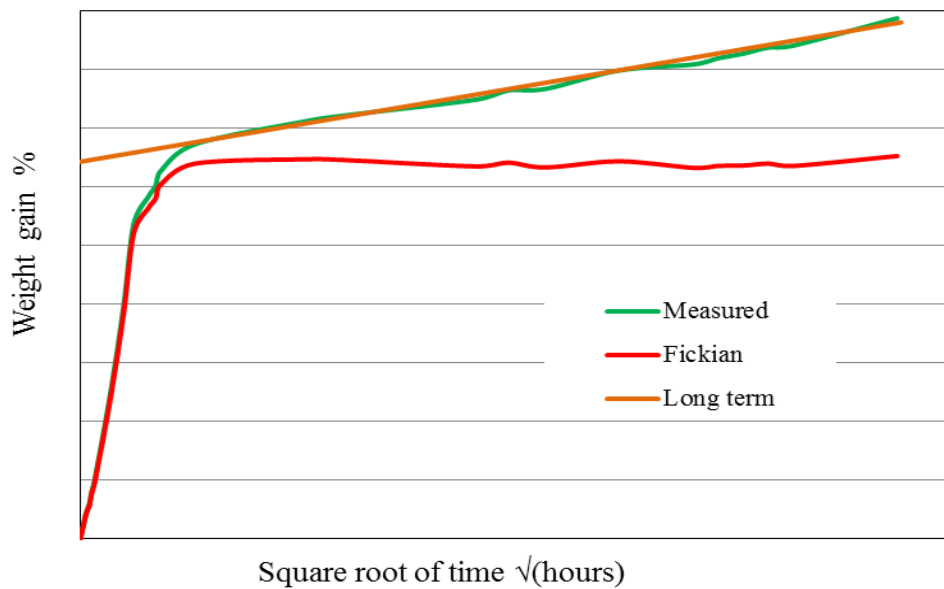


Figure 5. Extraction of Fickian behaviour from long term water uptake measurements

Table 2. Experimental directional diffusivities and saturation values of UD samples at various conditions

Condition	Saturation, weight %		Diffusion coefficients ,		
	Epoxy	Composite	$\times 10^{-14} \text{ m}^2/\text{sec}$		
23°C in water	3.7	1.36	$D_x=D_r$	D_y	D_z
40°C in water	3.8	1.35	12.1	4.8	2.3
70°C in water	3.95	1.34	32.0	13.1	5.0
70°C, 45% RH	0.7	0.35	141.4	71.9	22.6
70°C, 60% RH	1.1	0.6	186	91.9	32.6
70°C, 85% RH	2.4	1.08	185	70.8	25.8
			159	70.8	24.2

Moreover, the long term component is fitted reasonably well to a square root (time) behaviour, which might suggest a second diffusion process over a longer time scale. However if the increase in weight with long term immersion time was due to a relaxation-driven process then a different, exponential, behaviour would be expected. A combined relaxation / Fickian model can be applied to see if it is able to fit the data. This might enable the final water content and relaxation time constant to be estimated for a range of temperatures and humidities.

4.1.1 Diffusion coefficient

The moisture absorption as a function of time is given by the three-dimensional Fickian model, Equation 1.

$$\frac{\partial C}{\partial t} = D_x \frac{\partial^2 C}{\partial x^2} + D_y \frac{\partial^2 C}{\partial y^2} + D_z \frac{\partial^2 C}{\partial z^2} \quad (1)$$

Where C is the concentration, t the time and D_x , D_y and D_z are the diffusion coefficients.

For an infinite thin plate, the approximation for initial uptake or short term diffusion (up to about $M_t/M^* = 0.6$), is given by Equation 2:

$$\frac{M_t}{M^*} = \frac{4}{h} \sqrt{\frac{t \cdot D}{\pi}} \quad (2)$$

Where M_t is the absorption at time t , M^* is the saturation and h is the plate thickness.

In composites, the fibres can act as a barrier to the absorbed water molecules, so when the diffusion is perpendicular to the fibres the diffusion path will be more convoluted than when the diffusion is along the fibres. To consider this directional diffusion behaviour and to account for diffusion from edges, four different methods were compared:

1. Extrapolation to zero thickness (Intercept).
2. Using correction factor, Equation 3, derived by Shen and Springer [17] and extended to the case of anisotropic diffusion by Bao and Yee [13].

$$f_{ss} = \left(1 + \frac{h}{l} \sqrt{\frac{D_y}{D_x}} + \frac{h}{w} \sqrt{\frac{D_z}{D_x}} \right) \quad (3)$$

3. Using another alternative approximation developed by Starink, Starink and Chambers [18], Equation 4.

$$f_{ssc} = 1 + 0.54 \frac{h}{l} \sqrt{\frac{D_y}{D_x}} + 0.54 \frac{h}{w} \sqrt{\frac{D_z}{D_x}} + 0.33 \frac{h^2}{l.w} \sqrt{\frac{D_z D_y}{D_x^2}} \quad (4)$$

4. The full 3-D solution to the Fickian equation with anisotropic diffusion coefficients, Equation 5 [19].

$$G_{3D} = \frac{M_t}{M^*} = \left[1 - \left(\frac{8}{\pi^2} \right)^3 \sum_{i=0}^{\infty} \sum_{j=0}^{\infty} \sum_{k=0}^{\infty} \frac{1}{((2i+1)(2j+1)(2k+1))^2} \exp \left[-\pi^2 t \left[D_x \left(\frac{2i+1}{l} \right)^2 + D_y \left(\frac{2j+1}{w} \right)^2 + D_z \left(\frac{2k+1}{h} \right)^2 \right] \right] \right] \quad (5)$$

Detailed explanation of using these approximation methods can be found in other papers [11, 20] which concluded that the use of the Starink, Starink and Chambers (SSC) model is in close agreement with the full 3-D one. The Shen and Springer (S&S) approximation was shown to give systematically low values for diffusion across and through the fibres because it considers diffusion from all faces of a rectangular block, but does not take account of diffusion at edges or corners. The full 3-D analysis of diffusion is normally a time consuming computation, so the SSC method for determining the diffusivity for all conditions was used to obtain values for comparison with model outputs. It was clear that the key part to this is good experimental data and the use of repeat samples to average any differences in V_f and fibre geometry between samples. The diffusivity was noticed to vary with fibre orientation, where there is definitely lower diffusion through thickness than along layers. Resin diffusivity (D_r) was obtained assuming that diffusion is the same in all directions. The saturation and diffusivity values for resin and composite specimens

were determined to be used for the modelling and they are given in Table 2. D_x was assumed to be the same as D_r .

5. Modelling of directional diffusion in composites

Directional diffusion coefficients can also be derived by fitting experimental weight uptake curves to either the full 3-D Fickian solution or to FE models of 3-D diffusion [15, 19]. The effective diffusivity in composites with impermeable fibres has been examined by many researchers by using 3D finite element analysis on a fibre matrix unit cell [6, 21-24]. The aim in this section was to develop a finite element model to predict the Fickian diffusion of water into unidirectional carbon fibre/epoxy composites with varying temperatures and humidity.

5.1 Multi-scale structure

For modelling purposes, optical microscopy was used to characterize the composite specimens structure. The optical microscope images of these materials, Figure 6 top, showed yarns (tows) of fibre-rich regions with very high volume fraction of fibres embedded in the epoxy resin. The yarns were measured to be about 225 μm thick, and the resin layers between them approximately 10% of that. The average fibre diameter was 5.7 μm . Fibre volume fraction ($V_{f, \text{fibre}}^f$) within the yarns was measured by counting the number of fibres in three representative fibre-rich areas and calculating the corresponding area and hence volume fraction. This gave $V_{f, \text{fibre}}^f = 75\%$ for these regions. Due to the difference in the architecture of these composites, the success of the finite element model depends on how realistically the geometry of the sample architecture is modelled and

how well the effective properties of the different fibre regions are determined. It has been found that at the level of individual fibres, the predicted diffusivity of a unit cell depends significantly on the fibre volume fraction and arrangement, which have an effect on the gap size between fibres and the path length of diffusion through the matrix. Modelling using a regular fibre distribution has been found to give higher diffusivity than a random fibre distribution which has smaller gaps and longer diffusion paths [24]. Random distributions of fibres have been found to give results closer to measured data [22,25]; therefore fibres in the design step were randomly distributed.

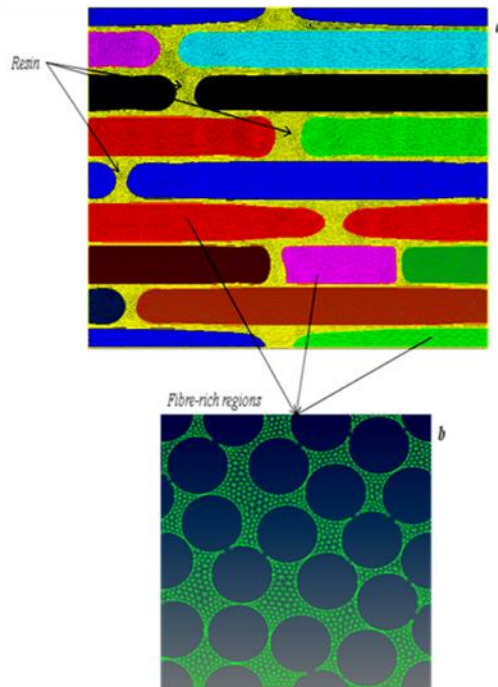
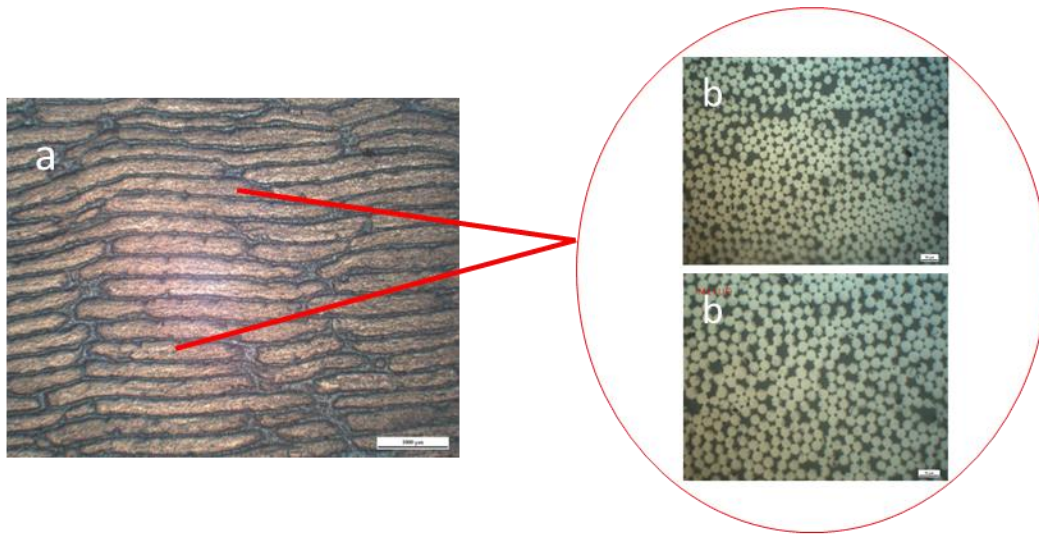


Figure 6. Cross section of UD composite (a) 20x magnification showing fibre-rich regions separated by resin layers, and (b) 800x magnification of a fibre-rich region (top). UD carbon fibre/M21 epoxy composite structures at two scale modelling (bottom)

5.2 Composite diffusivity prediction

The first stage of the modelling was to predict the three directional diffusion coefficients. Fibres were assumed to be parallel in the x-direction, so that D_x was assumed to be the same as that for the resin. 2D modelling could then be carried out in the y-z plane only. The second stage was to carry out 3D modelling to predict the water uptake curve for a “real” sample. Due to this complicated structure of these materials, the modelling was performed at three scales. At the microscale, circular fibres were randomly placed within a square unit cell. At the mesoscale, TexGen (a textile modelling package) was used for designing the geometry of the yarn structure [26]. For the whole composite sample, simple box geometry applied. At all scales, Hypermesh (a finite element analysis package) was used to mesh the structure with triangular or tetrahedral elements because these can more accurately represent the geometry between closely packed fibres and yarns [27]. Figure 6 (bottom) shows the micro- and meso- scales designed and FE meshed according to the first two steps. Finally, the outputs from the above packages were combined with an in-house modelling program for liquid diffusion. The computer model used to predict moisture diffusion was a Finite Element code based on the Fickian diffusion model and written in FORTRAN 95, which could run in either 2D or 3D using 3- or 4- node elements based on the methods described in Smith and Griffiths [28]. The model equations and boundary conditions are detailed below:

5.2.1 Saturation equation

Equation (6) was applied to calculate the saturation moisture content M^* (kg/m³) of the composite depending on the fibre volume fraction.

$$M^*_{yarn} = (1-V_{f,fibre})M^*_{epoxy} + V_{f,fibre} M^*_{fibre}$$
$$M^* = (1-V_{f,yarn})M^*_{,epoxy} + V_{f,yarn} M^*_{yarn} \quad (6)$$

In the case of micro-scale, i.e. fibres and resin within a yarn, $V_{f,fibre}$ is the volume fraction of fibres within the yarn, and since the carbon fibres don't absorb any water, $M^*_{fibre}=0$. At the meso-scale, i.e. yarns within the composite, $V_{f,yarn}$ is the volume fraction of yarns within the composite and M^*_{yarn} is the saturation moisture content within a yarn.

5.2.2 Diffusion Equation

Equation (7) was implemented using [P] the three dimensional permeability tensor = M* [D] (kg/m/sec) [23-25]. The continuous relative concentration $C^* = C/ M^*$ was used to address the complexity at material boundaries, between yarns and resin, where the concentration is discontinuous.

$$\nabla^T [P] \nabla C^* - \frac{\partial}{\partial t} C^* = 0 \quad (7)$$

Solving the finite element representation of this equation was carried out using a pre-conditioned conjugate gradient method [20].

5.2.3 Boundary conditions

The boundary conditions used in this study are:

1- The geometry and nodes of each face were forced to be identical to those on the opposite face without the need for the internal cells to be symmetrical. This enabled the modelling of a semi-infinite plate.

2- At the first two scales to predict the directional diffusion coefficients:

2.1. For diffusion in one- direction, boundary conditions were applied to mimic an infinite plate in the other two directions. For example, if diffusion is in z- direction then the relative concentration at each node on the “minimum “y” face was forced to be equal to that at the node directly opposite on the “maximum “y” face.

2.2. Steady state diffusion through the sample was modelled by setting the concentration on the ingoing and outgoing faces at saturation and zero respectively.

2.3. At steady state, an effective diffusivity (D_{eff}) was calculated using Fick’s first law to the sample as a whole and to individual elements, from Equation 8.

$$D_{eff} = \left(\frac{h}{M^*} \right) \langle [P] \{ \nabla C^* \} \cdot \{ n \} \rangle \quad (8)$$

$\{ n \}$ is the vector in the diffusion direction, and $\langle \rangle$ signifies a volume average.

This averages the flux over all elements and so takes account of inhomogeneity in the sample [20].

3- For modelling the whole sample, a one-eighth size box was used with saturation concentration on three orthogonal faces and a reflective boundary condition on each opposite face.

6. Modelling results and validation

In order to validate the model, diffusion coefficients and equilibrium moisture content derived from the water absorption experiments on the unfilled resin were fed into the model, and comparison of the predicted and measured water uptake curves for the composite and comparison of predicted and measured diffusivity in the y, and z- directions were carried out. Firstly, the value $D_{yz1(predicted)}$ was obtained from a unit cell with individual fibres representative of the fibre-rich regions of the composite, with a typical $V_{f, fibre}^f$ of 0.75. Since the micrographs showed no obvious difference between the y- and z- directions, a single diffusion coefficient could be used in this case. This is shown in Figure 7a which shows the fibre-rich structure with colours indicating the concentration profile at steady state when diffusion was in the y- and z- directions. Fibre-rich yarns, with $D_x=D_r$, $D_{y,yarn}=D_{z,yarn}=D_{yz1(predicted)}$ were then embedded in resin in a structure representative of the whole composite, as shown in Figure 7b. This also shows the concentration profile for diffusion in the y- and z-direction at steady state.

Diffusivities $D_{y,composite}$ and $D_{z,composite}$ were calculated, table 3. For the Fickian diffusion modelled, the predicted ratios $D_{y,composite}/D_r$ and $D_{z,composite}/D_r$ were determined by the unit cell geometries, table 4, and predicted ratios are very close therefore the averages were determined for all conditions. Measured values were then compared with averaged ratios, Figure 8. It can be seen that a close match to the average was achieved.

Table 3. Predicted diffusivities at the two scales of modelling of M21 UD specimens

		Fibre rich unit cell	M21 UD Composites	
Condition	$D_r = D_x$	$D_{yz1, Predicted}$	$D_{y, composite}$	$D_{z, composite}$
	Diffusion Coefficients $D(x10^{-14} \text{ m}^2/\text{s})$			
23 °C / Water	12.1	1.85	5.33	1.93
40 °C / Water	32.0	4.90	14.1	5.11
70 °C / Water	141	21.7	62.5	22.6
70 °C / 45%RH	186	28.6	82.3	29.9
70 °C / 60%RH	185	28.3	81.5	29.5
70 °C / 85%RH	159	24.4	70.3	25.5

Table 4. Predicted ratios $D_{y, composite}/D_r$ and $D_{z, composite}/D_r$ for the UD CF/M21 composite

Condition	$D_{y, composite}/D_r$	$D_{z, composite}/D_r$
23 °C / Water	0.44	0.159
40 °C / Water	0.44	0.159
70 °C / Water	0.443	0.160
70 °C / 45%RH	0.442	0.161
70 °C / 60%RH	0.441	0.159
70 °C / 85%RH	0.442	0.160
AVERAGE	0.441	0.160

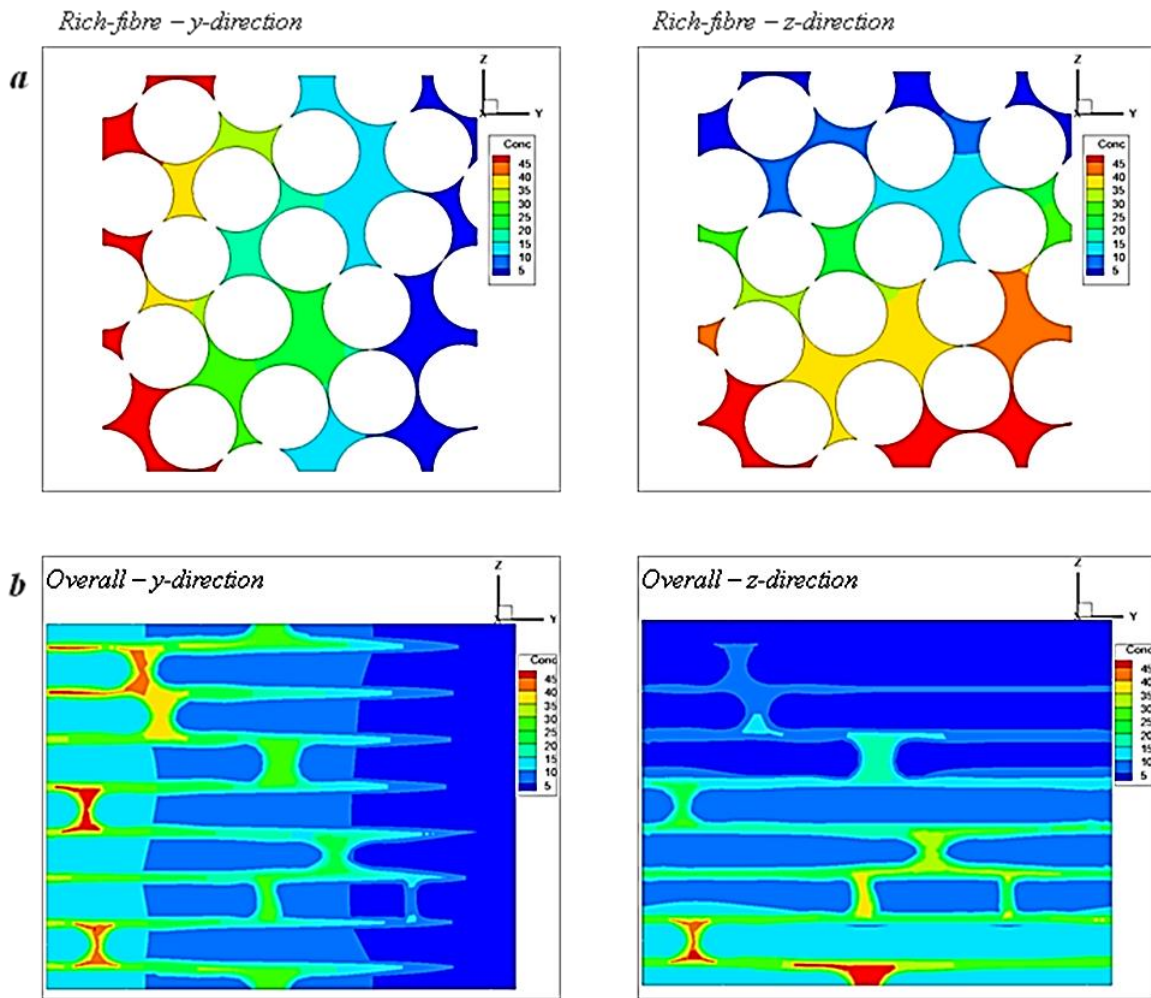


Figure 7. a) Fibre / resin arrangement representing rich-fibre regions in UD composite structure (b) represents the overall UD M21 composite structure(bottom). All figures have a concentration profile for y- and z-direction diffusion at steady state.

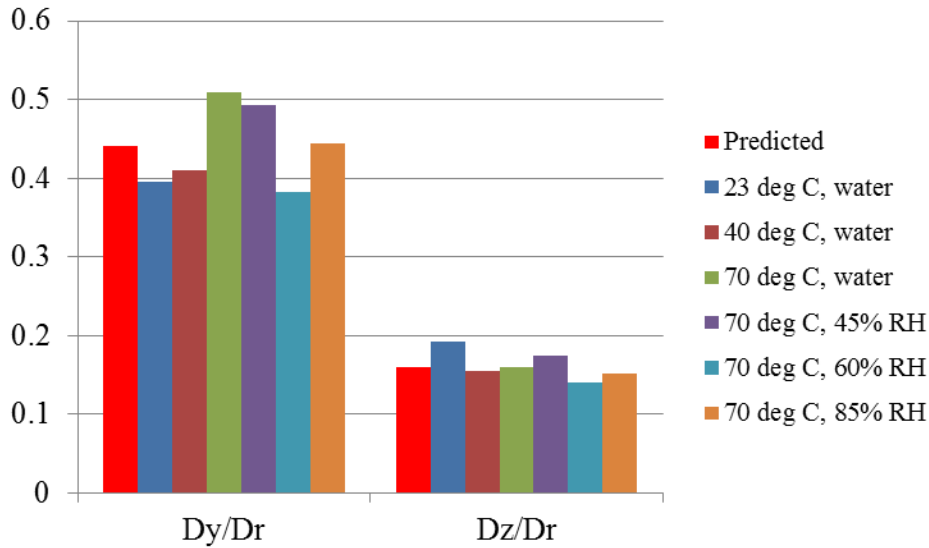


Figure 8. Comparison of averaged predicted ratios D_y/D_r and D_z/D_r with measured values for the UD CF/M21 composite.

Finally, the moisture uptake curve for the whole sample was predicted. Figure 9 shows the comparison between the experimental and the predicted weight uptake curves. The graphs show a close match between the measured and predicted curves. The predicted curves also showed that longer time is needed to reach saturation in the case of diffusion through the thickness. This may be attributed to the complex diffusion path where water has to go around the fibre compared to the diffusion along the fibre where the diffusion path is straightforward. It should be mentioned here that the average concentration at the initial value of all predicted moisture uptake curves was noticed to be slightly greater than zero (red circle), Figure 9. This is because the face nodes were initially at saturation and the weight gain percent was calculated as the volume average over the whole sample. Making the element finer would reduce the initial value to be closer to zero, but this was

not included in this study due to the massive number of elements that would be produced using very fine elements and the restrictions of the computer address space.

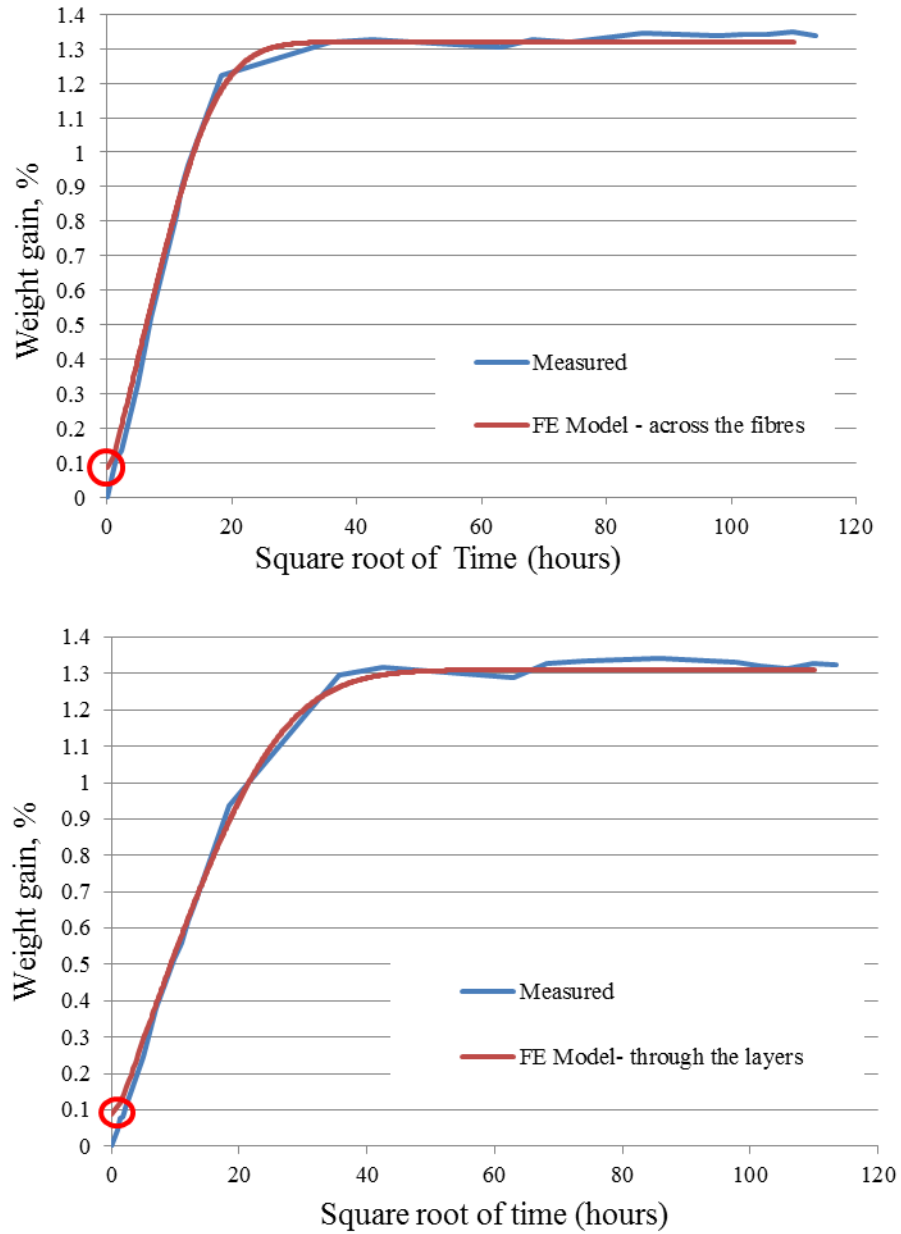


Figure 9. Comparison of predicted and measured water uptake curves for specimens (2mm thickness) conditioned at 70 °C / water across the fibres (top) and through the layers (bottom)

7. Conclusion

Water diffusion measurements of carbon fibre / epoxy composites with different fibre orientations showed that the diffusivity across fibres and through the thickness is smaller than along the fibres by factors of about 2-3 and 3-7, respectively. This can be attributed primarily to longer and more complicated diffusion paths across fibres and through the thickness of fibres. Diffusion rate also showed a dependency on the thickness of the samples where the diffusion rate decreased with increasing the thickness.

It was also found that extraction of Fickian behaviour, scaling by sample density as an approximate measure of the fibre volume fraction for obtaining saturation, and using the Starink, Starink and Chambers edge correction factor for deriving diffusivity are the best combination of methods to determine the saturation values and diffusivity needed for modelling. It has also been found that multi-scale modelling, starting from the behaviour at the level of individual fibres followed by larger scale models, can be used to derive the diffusion properties of representative unit cells. Validation of model predictions against experimental results showed that a close match between experimental and predicted ratios D_y/D_r and D_z/D_r . Predicted and measured water uptake curves were also in a good agreement. Therefore, it can be said that moisture absorption behaviour could be obtained using a reasonable representation of the microstructure. This representation of the detailed microstructure is a critical factor in the diffusivity prediction, and future work will further investigate the model sensitivity in this area.

8. References

1. W. R. Broughton and A. S, "Accelerated environmental aging of polymeric materials". A national measurement good practice guide No 103. National Physical Laboratory, Middlesex, UK (2007).
2. V. M. Karbhari and C. Xian C, *Composites B*, **40**, 41 (2009).
3. A. Chateauminois, L. Vincent, B. Chabert, and J. P. Soulier (1994), *Polymer*, **35**, 4766 (1994).
4. J. Zhou and J. P. Lucas, *Compos Sci Technol*, **53**, 57 (1995).
5. Y. Arao, J. Koyanagi, H. Hiroshi, et al, *16th International Conference on Composite Materials*, Koyoto, Japan, 8 July-13 July, 6 (2007).
6. Y. Aoki, K. Yamada, and T. Ishikawa, *Compos. Sci. Technol*, **68**, 1376 (2008).
7. H. S. Choi, K. J. Ahn, J. D. Nam, et al, *Composites Part A.*, **32**, 709 (2001).
8. H. Ardebili, C. Hillman, P. McCluskey, M. G. Pecht, and D. Peterson, *IEEE Transaction on Components and Packaging Technologies*, **25**, 132 (2002).
9. R. J. Morgan, E. O'Neal, D. L. Fanter, *J. Mater. Sci*, **15**, 751 (1980).
10. L. Kumosa, B. Benedikt, D. Armentrout, and M. Kumosa, *Composites A*, **35**, 1049 (2004).
11. J. C. Arnold JC, S. M. Alston, and F. Korkees, *Composites: Part A.*, 55, 120 (2013).
12. A. T. Dibenedetto, and P. J. Lex, *Polym. Eng. Sci.*, **29**(8), 543 (1989).
13. L. R. Bao, and A. F. Yee, *Polym. J.*, 43, 3987 (2002).
14. R. G. C. Arridge, and J. H. Speake, *Polym. J.*, **13/9**, 450 (1972).
15. T. K. Tsotsis, and Y. Weitsman Y, *J. Mater. Sci. Lett.*, **13**, 1635 (1994).
16. C. L. Leung, P. J. Dynes, and D. H. Kaelble., *ASTM STP.*, **696**, 298 (1979).
17. C. Shen, and G. S. Springer, *Environmental effects on Composite Material.*, **3**, 15 (1988).
18. M. J. Starink, L. M. P. Starink, and A. R. Chambers, *J. Mater. Sci.*, **37**, 287 (2002).
19. L. R. Grace and M. C. Altan, *Composites Part A.*, **43**, 1187 (2012).
20. S. Alston, F. Korkees, and C. Arnold, *ECCM15 - 15TH European Conference on Composite Materials, Venice, Italy, 24 June- 28 June*, pp.24-28 (2012).
21. L. Kumosa, B. Benedikt, D. Armentrout, et al, *Composites Part A.*, **35**, 1049 (2004).
22. P. Vaddadi, T. Nakamura, and R. P. Singh RP, *Acta. Materialia.*, **51**, 177 (2003).
23. J. Whitcomb, and X. Tang, *J. Compos. Mater.*, **36**, 1093 (2002).
24. K. Kondo, and T. Taki, *J. Compos. Mater.*, **16**, 82 (1982).

25. X. Tang, J. D. Whitcomb, Y. Li, et al, *Compos. Sci. Technol.*, **65/6**, 817 (2005).
26. University of Nottingham. Texgen open source software, http://texgen.sourceforge.net/index.php/Main_Page (2010, accessed 07 June 2016).
27. Altair Hyperworks Engineering Inc. Altair Hypermesh, <http://www.altairhyperworks.com> (2010, accessed 07 June 2016).
28. I. M. Smith, and D. V. Griffiths, *Programming the Finite Element Method*, 3rd ed, John Wiley & Sons, New Jersey, USA (1998).